The Journal of Clinical Endocrinology & Metabolism, 2020, Vol. 105, No. 12, e4459–e4473
doi:10.1210/clinem/dgaa616
Clinical Research Article

Clinical Research Article

RNA Sequencing and Somatic Mutation Status of Adrenocortical Tumors: Novel Pathogenetic Insights

Guido Di Dalmazi,[1,*] Barbara Altieri,[2,*] Claus Scholz,[3] Silviu Sbiera,[2] Michaela Luconi,[4] Jens Waldman,[5] Darko Kastelan,[6] Filippo Ceccato,[7] Iacopo Chiodini,[8,9] Giorgio Arnaldi,[10] Anna Riester,[11] Andrea Osswald,[11] Felix Beuschlein,[11,12] Sascha Sauer,[13] Martin Fassnacht,[2] Silke Appenzeller,[14,*] and Cristina L. Ronchi[2,15,*]

[1]Endocrinology Unit, Department of Medical and Surgical Sciences, University of Bologna, Italy; [2]Division of Endocrinology and Diabetes, Department of Internal Medicine I, University Hospital, University of Würzburg, Würzburg, Germany; [3]Life and Medical Sciences Institute, University of Bonn, Germany; [4]Department of Experimental and Clinical Biomedical Sciences, University of Florence, Italy; [5]Mivendo Klinik Hamburg, Germany; [6]Department of Endocrinology, University Hospital Center Zagreb, Croatia; [7]Endocrinology Unit, Department of Medicine DIMED, University-Hospital of Padua, Italy; [8]Istituto Auxologico Italiano, IRCCS, Unit for Bone Metabolism Diseases and Diabetes & Lab of Endocrine and Metabolic Research, Milan, Italy; [9]University of Milan, Milan, Italy; [10]Division of Endocrinology, Department of Clinical and Molecular Sciences, Polytechnic University of Marche, Ancona, Italy; [11]Medizinische Klinik und Poliklinik IV, Klinikum der Universität München, Munich, Germany; [12]Klinik für Endokrinologie Diabetologie und Klinische Ernährung, Universitäts Spital Zürich, Zürich, Switzerland; [13]Max Delbrück Center for Molecular Medicine/Berlin Institute of Health, Berlin, Germany; [14]Core Unit BioinformaticFsupps, Comprehensive Cancer Center Mainfranken, University of Würzburg, Germany; and [15]Institute of Metabolism and Systems Research, University of Birmingham, United Kingdom

ORCiD numbers: 0000-0003-2616-3249 (B. Altieri); 0000-0002-6271-5533 (S. Sbiera); 0000-0001-7594-3300 (I. Chiodini); 0000-0001-7826-3984 (F. Beuschlein); 0000-0001-6170-6398 (M. Fassnacht); 0000-0001-5020-2071 (C. L. Ronchi).

*Authors contributed equally to the work.

Abbreviations: ACA, adrenocortical adenoma; ACC, adrenocortical carcinoma; ACTH, adrenocorticotropin; cAMP, cAMP 3′,5′-cyclic adenosine 5′-monophosphate; CPA, cortisol-producing adenoma; CS, Cushing syndrome; DST, dexamethasone suppression test; EIA, endocrine-inactive adenoma; FPKM, fragments per kilobase of transcript per Million mapped reads; lncRNA, long noncoding ribonucleic acid; MACS, mild autonomous cortisol secretion; NAG, normal adrenal gland; PCA, principal component analysis; PCR, polymerase chain reaction; PKA, protein kinase A; RNA, ribonucleic acid; UFC, urine free cortisol; WES, whole-exome sequencing.

Received: 6 May 2020; Accepted: 28 August 2020; First Published Online: 1 September 2020; Corrected and Typeset: 6 October 2020.

Abstract

Context: Pathogenesis of autonomous steroid secretion and adrenocortical tumorigenesis remains partially obscure.

Objective: To investigate the relationship between transcriptome profile and genetic background in a large series of adrenocortical tumors and identify new potential pathogenetic mechanisms.

Design: Cross-sectional study.

ISSN Print 0021-972X ISSN Online 1945-7197
Printed in USA

Setting: University Hospitals of the European Network for the Study of Adrenal Tumors (ENSAT).
Patients: We collected snap-frozen tissue from patients with adrenocortical tumors (n = 59) with known genetic background: 26 adenomas with Cushing syndrome (CS- cortisol-producing adenoma [CPA]), 17 adenomas with mild autonomous cortisol secretion (MACS-CPAs), 9 endocrine-inactive adenomas (EIAs), and 7 adrenocortical carcinomas (ACCs).
Intervention: Ribonucleic acid (RNA) sequencing.
Main Outcome Measures: Gene expression, long noncoding RNA (lncRNA) expression, and gene fusions. Correlation with genetic background defined by targeted Sanger sequencing, targeted panel- or whole-exome sequencing.
Results: Transcriptome analysis identified 2 major clusters for adenomas: Cluster 1 (n = 32) mainly consisting of MACS-CPAs with *CTNNB*1 or without identified driver mutations (46.9% of cases) and 8/9 EIAs; Cluster 2 (n = 18) that comprised CP-CPAs with or without identified driver mutation in 83.3% of cases (including all CS-CPAs with *PRKACA* mutation). Two CS-CPAs, 1 with *CTNNB*1 and 1 with *GNAS* mutation, clustered separately and relatively close to ACC. lncRNA analysis well differentiate adenomas from ACCs. Novel gene fusions were found, including *AKAP*13-*PDE*8*A* in one CS-CPA sample with no driver mutation.
Conclusions: MACS-CPAs and EIAs showed a similar transcriptome profile, independently of the genetic background, whereas most CS-CPAs clustered together. Still unrevealed molecular alterations in the cAMP/PKA or Wnt/beta catenin pathways might be involved in the pathogenesis of adrenocortical tumors.

Freeform/Key Words: adrenocortical adenoma, Cushing syndrome, mild autonomous cortisol excess, transcriptome, gene fusions, long non-coding RNA

Over the last few years, the molecular and genetic events underlying the pathogenesis of adrenocortical tumors have been investigated by applying classical genetic approaches and next-generation sequencing techniques including whole-exome sequencing (WES). Alterations of several components of the cAMP/PKA pathway have been identified as a causative factor for tumorigenesis and cortisol hypersecretion in adrenocortical adenoma (ACA) (reviewed in (1, 2)). Independent studies have reported somatic mutations in the *PRKACA* gene as the pivotal pathogenetic event in approximately half of the ACAs associated with Cushing syndrome (CS), due to a constitutive activation of the catalytic subunit α of protein kinase A (PKA) (3-7). In a smaller proportion of patients with CS, additional mutations in members of the 3′,5′-cyclic adenosine 5′-monophosphate (cAMP)/PKA signaling pathway have newly been described, such as somatic mutations of the gene encoding the catalytic subunit beta of PKA (*PRKACB*, very rare) (8), or confirmed, such as those occurring in the gene encoding the regulatory subunit 1 α of PKA (*PRKAR*1*A*) or in the catalytic α subunit of PKA or the protein Gsα (*GNAS*) (4, 5, 7, 9, 10). Activating mutations in the gene encoding β-catenin (*CTNNB*1) have also been identified as an important contributor of adrenocortical growth. Interestingly, *CTNNB*1 mutations had been reported in ACA and adrenocortical carcinoma (ACC) with a similar prevalence (10-30%) (9, 11) with the highest frequency in endocrine inactive adenomas (EIAs) (9, 12). Despite these substantial advances, the molecular mechanisms underlying autonomous steroid secretion and adrenocortical tumorigenesis remain obscure for around 2/3 of cases that cannot be linked to known driver mutations.

Another important issue is that, depending on the definition used, up to 40% of patients with apparently nonfunctioning ACA might present a mild autonomous cortisol secretion (MACS), a condition previously termed "subclinical CS," since the classical clinical manifestations of overt hypercortisolism are absent (13, 14). However, several evidences suggest that MACS could be associated with cortisol-dependent comorbidities, including higher risk of cardiovascular events, hypertension, dyslipidemia, diabetes mellitus type 2, obesity, osteoporosis, and higher mortality rate (13, 15-19). A previous study on transcriptome analysis on a small series of ACAs identified 2 different clusters according to hormone secretion: cluster 1, including only cortisol-producing adenomas (CPAs) associated with CS (CS-CPAs), and cluster 2 including nonfunctioning ACAs, as well as MACS- and CS-CPAs, revealing an association between cortisol secretion and expression of a subset of genes implicated in steroid secretion (20). However, as to this point, the association between transcriptome and mutational status of benign adrenocortical tumors has not been investigated.

Our first aim was to analyze the association between the genetic background and the transcriptome profile assessed

by ribonucleic acid sequencing (RNA-seq) in a large series of ACAs. Our second aim was to identify novel molecular events that may be involved in cortisol hypersecretion and adrenocortical tumorigenesis through the analysis of alternative gene spliced transcripts, long noncoding ribonucleic acids (lncRNAs), and gene fusions.

Materials and Methods

Study protocol

This is a European multicentric retrospective study among centers belonging to the European Network for the Study of Adrenal Tumors (ENSAT), designed and conducted in accordance with the Declaration of Helsinki. The local ethics committees of each Institution approved the study protocol. Written informed consent was obtained from all subjects prior to study enrollment.

Selection of patient cohort

We selected snap-frozen samples from the previously published series of 99 non-aldosterone producing ACAs without exon 7 hot-spot *PRKACA* mutations, already characterized by WES (9). Among these, we took 54 samples with still available tumor material for RNA isolation. After excluding 7 cases due to poor quality RNA (see "Sample preparation"), we obtained a final series of 47 ACAs for RNA-seq analysis (Fig. 1). According to the results of WES, we identified 22/47 (46.8%) ACAs with somatic mutations in known driver genes, such as *GNAS*, *CTNNB*1, and *PRKACA* (outside the hot-spot region). These included 7 CS-CPAs, 11 MACS-CPAs, and 4 endocrine inactive adenomas (EIAs). The remaining 25/47 (53.2%) tumors (n = 14 CS-CPAs, 6 MACS-CPAs, and 5 EIAs) did not have somatic mutations in known driver genes at WES. In addition, we included 5 further CS-CPAs samples with known hot-spot L206R *PRKACA* mutations from the previously published cohort (6) and 7 early-stage/low aggressive ACCs (ENSAT tumor stage 1-3, Ki67 proliferation index <20%), among which 5 were previously analyzed by targeted panel next generation sequencing (21). Additionally, 4 normal adrenal glands (NAGs) obtained from surgery for renal carcinoma (n = 1) or from tissue surrounding EIA (n = 3) were used as controls for gene expression profiling. The dissection of the adrenal tissues from the snap-frozen specimen was made by expert pathologists at each center participating in the study. The final cohort comprised 63 samples, including 59 adrenocortical tumors (Fig. 1). By performing variant calling on our RNA-seq data (see "Material and Methods"), we could detect 2 additional somatic mutations in 2 CS-CPA cases classified as without driver mutations based on previous WES results. These mutations were in genes *PRKACA* (hot-spot p.L206R found in CS-CPA2) and *GNAS* (hot-spot p.R201S in CS-CPA6) (all supplementary material and figures are located in a digital research materials repository; Supplementary Table 1 (22)). Moreover, 2 previously identified alterations in *CTNNB*1 genes could not be verified, a 1602 bp splice indel in CS-CPA22 and a missense mutation *CTNNB*1 p.T41A in MACS-CPA9. According to these findings, we finally classified our cohort as follows (Fig. 1): 27 ACA with known driver mutations (7 CS-CPA_PRKACA, 4 CS-CPA_GNAS, 2 CS-CPA_CTNNB1, 9 MACS_CTNNB1, 1 MACS-CPA_GNAS, 4 EIA_CTNNB1) and 25 ACAs

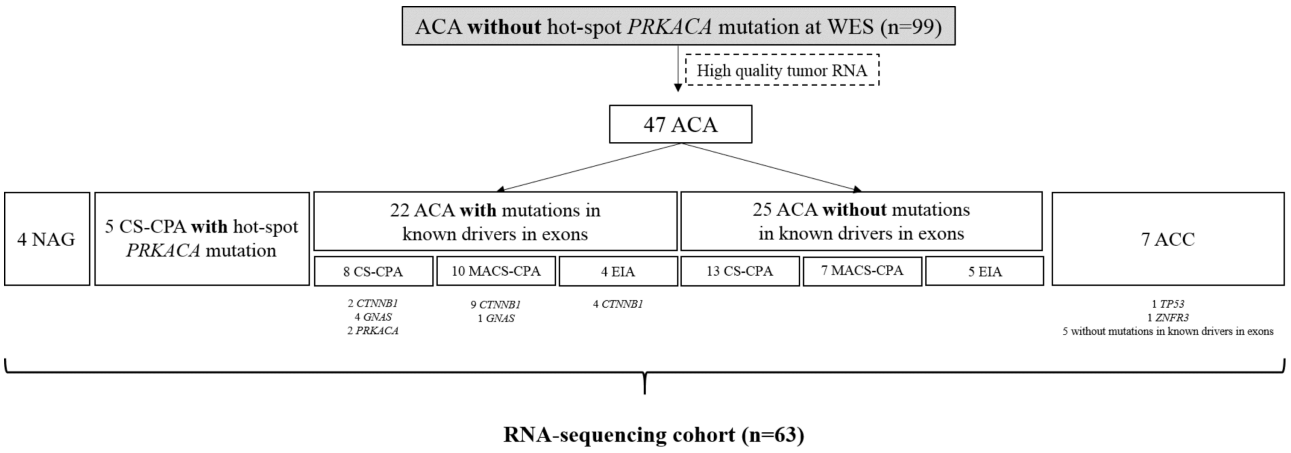

Figure 1. Flow-chart of the selection process of adrenocortical tumor samples. Samples were classified according to diagnosis and to the presence of driver mutations based on the previous whole-exome sequencing (WES) (9), targeted sequencing, and on the new variant calling from RNA-seq data. ACA, adrenocortical adenomas. NAG, normal adrenal glands. CS-CPA, cortisol-producing adenomas with overt Cushing Syndrome. MACS-CPA, cortisol-producing adenomas with mild autonomous cortisol secretion. EIA, endocrine-inactive adenoma. ACC, adrenocortical carcinoma.

without driver mutations (13 CS-CPAs, 7 MACS-CPAs, and 5 EIAs).

Clinical data collection

Clinical and hormonal data of ACA patients, such as sex, age at diagnosis, initial tumor size, steroid secreting pattern, and symptoms of overt CS, were available from previous studies (6, 9).

Overt CS and MACS were defined according to the Endocrine Society guidelines (14), in order to maintain the same classification of previous studies (6, 9). These guidelines recommend the use of the 1 mg overnight dexamethasone test (DST) with a cortisol cutoff of <1.8 µg/dL (50 nmol/L) as the primary test to exclude autonomous cortisol secretion. However, the newest European Society of Endocrinology (ESE)/ENSAT guidelines from 2016 (13) recommend interpreting the 1-mg overnight DST as a continuous variable, considering postdexamethasone serum cortisol levels between 1.9 and 5.0 µg/dL (51 and 138 nmol/L) as "possible autonomous cortisol secretion" and levels >5.0 µg/dL (>138 nmol/L) as confirmed "autonomous cortisol secretion." Both guidelines recommend the use of additional biochemical tests to confirm cortisol secretory autonomy and assess the degree of cortisol secretion, and MACS were defined in absence of clinical and catabolic signs of overt CS (13, 14). To avoid bias in the interpretation of our results, we performed a second analysis classifying the patients according to the ESE/ENSAT guidelines. According to that, 2 MACS-CPAs (MACS-CPA2 and MACS-CPA11) without driver mutation were reclassified as EIAs, and 1 EIA with *CTNNB*1 mutation (EIA6) was reclassified as MACS-CPA. Differences between the results deriving from the 2 classifications were evaluated. In all our patients with MACS-CPA with values between 1.8 and 5 µg/dL, adrenocorticotropin (ACTH) was below 2.2 pmol/L (10 pg/mL) or midnight cortisol was above the reference range.

Clinical and histopathological data of ACC cases, including ENSAT tumor stage, Weiss score, and Ki67 index, were available from a previous publication in 5 out 7 cases (21) or were collected through the ENSAT registry in the remaining 2 samples (https://registry.ensat.org/).

Sample preparation and RNA-sequencing

RNA was isolated from snap-frozen tumor tissue by RNEasy Lipid Tissue Mini Kit (Qiagen, Hilden, Germany) (n = 23) or by Maxwell® 16 Total RNA Purification Kit used with the Maxwell® 16 Instrument (n = 36), according to the manufacturers' instruction. Initial RNA quality control was performed by spectrophotometry at 260 nm and by running a denaturing agarose gel. Additional analysis was performed using an Agilent Technologies 2100 Bioanalyzer and an RNA Integrity Number value ≥8 was required to ensure efficient mRNA sequencing.

TruSeq RNA Library Prep Kits was applied prior Illumina sequencing (NextSeq500) of pooled normalized libraries. Specifically, a paired-end 75 nt mode (high-output flow cells) was used for a minimum of 40 to 100 million reads per sample.

Data analysis

An initial quality assessment was performed using FastQC, v0.11.5 (Available online at: http://www.bioinformatics.babraham.ac.uk/projects/fastqc). Adapter and quality trimming was done with Cutadapt, v1.1.5 (23). STAR v2.5.3a (24) was used to map the trimmed reads to the GENCODE human reference genome GRCh37 release 29. We used Samtools v1.3 (25) utilizing htslib, v1.3 for sam-to-bam conversions as well as sorting and indexing of the alignment files. For gene annotation, the GENCODE human reference genome GRCh37 release 29 was used. Fragments Per Kilobase of transcript per Million mapped reads (FPKM) values and differential gene expression as well as differential isoform expression were calculated with Cufflinks package, v2.2.1 (26). For principal component analysis (PCA) and creation of the heatmap, the value 1 was added to all FPKM values in order to make the following normalization step possible. FPKM values of all genes with a coefficient of variation ≥0.5 were normalized to the median FPKM of the 4 sequenced NAGs and $\log_2$-transformed ($\log_2$FoldChange). PCA was performed with the prcomp function from the R stats package, v3.4.4. Subsequently, 500 protein-coding genes and 250 lncRNA genes with the highest PC loadings in one of the first three components were selected for unsupervised complete linkage clustering, respectively. The clustering was performed on the rows and columns using the Euclidian distance metric with the heatmap.2 function in the gplots R-package, v3.0.1. Arriba v1.1.0 was used for fusion detection with default settings (https://github.com/suhrig/arriba/).

For pathway analysis, we used the Gene Set Enrichment Analysis (GSEA) software by Broad Institute v.MSigDB 7.0 (27, 28) using gene sets from both Reactome and KEGGS pathways.

Variant calling using RNAseq data

Variant calling was performed following the GATK Best Practices workflow for SNP and Indel calling on RNAseq data (https://software.broadinstitute.org/gatk/documentation/article.php?id=3891). Reads were trimmed

with TrimGalore, v06.6.1 (https://www.bioinformatics.babraham.ac.uk/projects/trim_galore/) utilizing Cutadapt, v2.3 (23) and mapped to the reference using STAR, v2.5.4b (24). The index and the dictionary of the reference sequence were created using Samtools v1.3 (25) and Picard, v2.18.11 (https://broadinstitute.github.io/picard/), respectively. Picard was also used to add read groups, to sort alignment files, to mark duplicates, and to create index files. The Genome Analysis Toolkit v3.8 (29) was used to reassign mapping qualities, indel realignment, base recalibration, variant calling, as well as variant filtering. Variants were annotated using ANNOVAR (v2019-10-24) (30). Somatic protein-altering variants and splice site variants in known ACC driver genes (*TP53* and *ZNFR3*) as well as known ACA driver genes (*CTNNB1*, *PRKACA* and *GNAS*) are reported if they alter the protein sequence or affect a splice site, are rare in the population (below a frequency of 2% in 1000g2015aug_all, ExAC_nontcga_ALL, gnomAD_exome_ALL and gnomAD_genome_ALL), and the position is covered by at least 20 reads and the alternative allele is covered by at least 8 reads and comprised at least 5% (Supplementary Table 1 (22)).

Validation of gene fusions

We selected a total of 7 high-confidence gene fusions to be validated by polymerase chain reaction (PCR) and Sanger sequencing. Reverse transcription of RNA was performed using the QuantiTect Reverse Transcription Kit (Qiagen, Hilden, Germany) as previously described (31). PCR amplification of 10 ng of cDNA was performed in a final volume of 25 µL using specific primer sets designed to span the fusion breakpoints, whereas *GAPDH* was used as internal control gene (Supplementary Table 2 (22)). Cycling conditions were 96°C for 2 minutes followed by 30 cycles of denaturing at 96°C (30 seconds), annealing at 58°C (30 seconds), elongation at 72°C (1 minute), and a final step of 72°C for 5 minutes. The PCR products were run on a 2.4% low-melt agarose gel with ethidium bromide. PCR products were purified (ExoSAP-IT, Amersham Biosciences, Munich, Germany) and sequenced using the QuickStart Cycle Sequencing Kit (AB Sciex, Beckman Coulter, #608120, Krefeld, Germany) on a Genetic Analysis System (CEQ) 8000 (AB Sciex, #A16637-AA, Krefeld, Germany) capillary sequencer according to the manufacturer instructions. Data were analyzed using the CEQ8000 DNA Analyzer (AB Sciex).

Statistical analysis

To correlate the results of the unsupervised clustering analysis with the clinical features, the following parameters were evaluated: sex, age (cut-off 50 years old), tumor size (cut-off 35 mm), diagnosis (EIA, MACS-CPA, CS-CPA, and ACC), and mutational status (no driver mutations, *CTNNB1* mutation, mutations of the cAMP/PKA pathway, other driver mutations). A Fisher exact or chi-squared (χ^2) tests was used to investigate dichotomic variables, while a 2-sided *t*-test or Mann–Whitney U test was used to compare continuous variables, as appropriate. The Kruskal–Wallis test, followed by Bonferroni post hoc test, or Dunn's multiple comparison test, was used for comparison among several groups for non-normally distributed variables. Correlations and 95% confidence intervals (95% CI) between different parameters were evaluated by linear regression analysis. Statistical analyses were made using GraphPad Prism (v.6.0, La Jolla, CA, USA) and SPSS Software (v.23, SPSS Inc., Chicago, IL, USA). Data are presented as median with interquartile range in parentheses or mean ± standard deviation (SD). $P < .05$ was considered statistically significant.

Results

Patient characteristics

Clinical parameters and hormonal levels at the time of diagnosis are reported in Table 1. Patients with CS-CPAs were mostly females and significantly younger than those of the other groups ($P < .005$). As expected, they had significantly higher post-dexamethasone cortisol levels and 24-hour urinary free cortisol, as well as lower ACTH levels in comparison to other groups (Table 1). No other significant differences were observed in clinical parameters.

Among ACCs, 2 patients had nonsecreting tumors and 5 had secreting ACC, including 2 overt Cushing, 1 MACS, and 2 with androgens excess.

Gene expression profile (overview)

The entire list of significantly differentially expressed protein-coding genes with log2 fold changes above 2 or below –2 is reported in the Supplementary Table 3 (22). Protein-coding genes recognized at RNA-seq represented 86% of all detected genes, whereas the remaining gene types included processed and unprocessed pseudogenes, mitochondrial rRNA, and lncRNA (Supplementary Figure 1 (22)). The number of significantly over- and underexpressed protein-coding genes in each group and the most frequently altered pathways are reported in Table 2. CS-CPAs showed 67 overexpressed genes, being mostly related to *GPCR* ligand binding and *G alpha* (q) signaling, with *NTS*, *TJP3*, *MMP7*, *ITIH1*, *GPRC6A*, *TNNT1*, *FATE1*, and *GIPR* among the top 40 genes. Conversely, MACS-CPAs and EIAs showed only few

Table 1. Clinical parameters, and hormonal and genetic data of patients with adrenocortical tumors

	EIA (n = 9)	MACS-CPA (n = 17)	CS-CPA (n = 26)	ACC (n = 7)
Clinical and hormonal parameters				
Age, years	59.0 (55.0-71.5)	57 (47-62)	41.5 (35.0-47.3)[c]	51.0 (47.0-60.0)
Females, n (%)	4 (44%)	13 (76%)	25 (96%)[c]	4 (57%)
Tumor size, cm	3.3 (2.1-5.2)	4.0 (3.4-4.5)	3.3 (2.8-3.6)	11.0 (8.5-15.0)
Post-dexamethasone cortisol, nmol/L (n.a.)	35.9 (24.8-63.4)	84.1 (75.2-168.3)[c]	449.7 (373.8-551.8)[c]	59.3 (36.5-539.4) (3)
24-h UFC, nmol/day (n.a.)	n.a.	568 (174-1060) (4)	1327 (682-2118)[d] (12)	105.3 (74.2-248.8) (2)
ACTH, pmol/L (n.a.)	5.1 (1.9-7.3) (4)	0.8 (0.4-1.8)[d] (1)	0.7 (0.2-1.1)[c] (11)	14.1 (3.0-33.3) (1)
Ki67 index, % – median (range)	n.appl.	n.appl.	n.appl.	10 (2-15)
Genetic data				
Number of somatic mutations[a] – median (range)	4 (1-15)	2 (0-17)	4 (0-40)	n.c.
Samples with known driver mutations[ab], n (%)	4 (44%) *CTNNB1* n = 4	11 (65%) *CTNNB1* n = 10 *GNAS* n = 1	12 (46%) *PRKACA* n = 6 *GNAS* n = 3 *CTNNB1* n = 3	2 (40%) *TP53* n = 1 *ZNRF3* n = 1

Data are expressed as median and interquartile ranges in parentheses, if not otherwise specified. CPA-CS, cortisol-producing adenoma associated with overt Cushing syndrome, CPA-MACS, cortisol-producing adenoma associated with mild autonomous cortisol secretions, EIA, endocrine inactive adenoma, ACC, adrenocortical carcinoma, n.a., number of patients with not available, n.appl., not applicable, UFC, urinary free cortisol.

Overt CS and MACS were defined according to the Endocrine Society guidelines (13).

[a]Number of somatic mutations were counted according to previously published data deriving from whole-exome sequencing (WES) for ACAs (9). ACCs were analyzed by targeted next generation sequencing (NGS) covering about 100 genes, including 5/7 cases deriving from a previous publication (21). Due to the huge difference of covered genes between WES and targeted (20.000 vs 100), the number of mutations between ACAs and ACCs are not comparable (n.c.). Moreover, only early-stage/low aggressive ACCs in this study, explains the very low number of found mutations (1 in *TP53* and 1 in *ZNFR3* gene).

[b]According to targeted sequencing of *PRKACA* exon 7 hot-spot mutations (6) or targeted next-generation sequencing for ACC (21).

[c]$P < .005$ vs EIA (Kruskall–Wallis test followed by Bonferroni).

[d]$P < 0.05$ vs EIA (Kruskall–Wallis test followed by Bonferroni); for 24-hour UFC MACS-CPA vs CS-CPA (Mann–Whitney test).

overexpressed genes (not enough for pathway analysis). ACCs samples presented 472 significantly overexpressed genes, mostly involved in cell cycle and mitosis. *DUSP9*, *PAX9*, *SULT1C2*, *PMAIP1*, *DHRS2*, *CPNE4*, *PBK*, and *DSG2*, but also *CDK1*, *BIRC7*, and *IGF2* were among the top 40 overexpressed genes. Underexpressed genes in ACCs, like *GNG4*, *GNB3*, *CAMK2B*, *ADCY2*, and *SLC17A7*, were observed mostly in transport of small molecules, neuronal system, and GPCR ligand binding.

Relationship between gene expression profile and mutational status

At subgroup 3D PCA (Fig. 2A) for protein-coding genes we could classify tumor samples in 4 groups: 1 group including all EIAs and all MACS-CPA with *CTNNB1* mutations or without mutation in a known driver gene, 1 group with MACS-CPA_GNAS and all CS-CPAs, except for the 2 CS-CPAs with *CTNNB1* mutations which show a gene expression pattern closer to ACCs than most of the remaining benign tumors, and ACCs. The individual 3D PCA plots for protein-coding genes in the entire cohort (52 ACA, 7 ACC, 4 NAG) is shown (see Supplementary Figure 2A (22)).

Unsupervised clustering analysis using the top 500 differentially expressed protein-coding genes (represented as heatmap in Fig. 2B and Supplementary Table 4 (22)) was performed. According to the heatmap, we could classify tumor samples in 4 clusters (Fig. 2B): (1) "Cluster 1" (n = 32), including EIAs and MACS-CPAs either with *CTNNB1* mutations (EIA_CTNNB1, n = 4, and MACS-CPA_CTNNB1, n = 9) or without mutation in a known driver gene (EIA_none, n = 4, and MACS-CPA_none, n = 6), CS-CPAs without known driver mutations (n = 7) or with *GNAS* mutation (n = 2); (2) "Cluster 2," comprising mostly CS-CPAs with or without driver mutation (CS-CPA_PRKACA, n = 7; CS-CPA_GNAS, n = 1; CS-CPA_CTNNB1, n = 1; and CS-CPA_none, n = 6), together with two MACS-CPAs (MACS-CPA_GNAS, n = 1, and MACS-CPA_no driver, n = 1) and one EIA_no driver; (3) 1 CS-CPA with *CTNNB1* mutations and 1 CS-CPA with *GNAS* mutation, which clustered separately from the other benign tumors; and (4) "ACC" (n = 7) clustering separately from all other groups.

Results from PCA and unsupervised clustering analysis did not change by classifying the adenomas according to the ESE/ENSAT guidelines (13), when considering all the

Table 2. Biological pathways in protein-coding genes differentially expressed in adrenocortical tumors according to phenotype

	Underexpressed genes		Over-expressed genes	
	Total n genes	Pathways	Total n genes	Pathways
CS-CPA (n = 26)	125	1) Regulation of Insulin-like Growth Factor (IGF) transport and uptake by Insulin-like Growth Factor Binding Proteins (IGFBPs)	67	1) GPCR ligand binding 2) G alpha (q) signaling 3) Peptide ligand-binding receptors 4) Class A/1 (Rhodopsin-like receptors) 5) Signaling by GPCR
MACS-CPA (n = 17)	338	1) Neuronal system 2) Muscle contraction 3) Transmission across Chemical Synapses 4) Cardiac conduction 5) Potassium channel	7	No pathways significantly represented among the overexpressed genes
EIA (n = 9)	243	1) Neuronal system 2)Transmission across chemical synapses 3) Neurotransmitter receptor binding	1	No pathways significantly represented among the overexpressed genes
ACC (n = 7)	591	1) Transport of small molecules 2) Neuronal System 3) GPCR ligand binding 4) Signaling by GPCR 5) Class B/2 (Secretin family receptors)	472	1) Cell cycle 2) Mitosis 3) Rho GTPase 4) Glucuronidation 5) Kinesins

CPA-CS, cortisol-producing adenoma associated with overt Cushing syndrome; CPA-MACS, cortisol-producing adenoma associated with mild autonomous cortisol secretions; EIA, endocrine inactive adenoma; ACC, adrenocortical carcinoma. Underexpressed genes by $\log_2$ fold change values >2 and over-expressed genes by $\log_2$ fold change values <–2. Pathway analysis was performed by GSEA (Gene sets from Reactome) and KEGGS.

differentially expressed genes. Therefore, further analyses were performed according the Endocrine Society guidelines (14).

The analysis of clinical data among clusters identified by mRNA gene expression showed significant differences in age (χ^2 = 10,13, P = .02), tumor size (χ^2 = 10.63, P = .01), diagnosis (χ^2 = 77.30, P < .001), and mutation status (χ^2 = 37.79, P < .001) (Fig. 2B). No significant difference among the clusters were observed in sex (χ^2 = 5.87, P = .12). Patients in Cluster 1 were older (61.3% of the cases had ≥55 years) and had larger tumors (58.1% of the cases had tumors ≥35 mm) either inactive (all but 1 inactive tumors grouped in Cluster 1) or associated with MACS (46.9% of cases). Except 2 CPAs, all remaining tumors with *CTNNB*1 somatic mutations were also included in Cluster 1 (Fig. 2B). On the contrary, in Cluster 2, all patients, except 1 were female, with diagnosis of overt CS in 15/18 (83.3%) cases, among which 77% of cases had <55 years. Mutations in the cAMP/PKA pathway or unknown driver mutations were found in 50.0% and 44.4% of cases, respectively. The 3 cases that were not CS-CPAs belonging to Cluster 2 were 1 EIA and 2 MACS-CPAs. The single EIA_no driver (EIA8) was a 44-year-old female patient, with a right adrenal tumor of 2.8 cm and no signs of hormone secretion, including suppressed cortisol post-DST (<27.59 nmol/L), and 24-hour urine free cortisol (UFC) and ACTH levels within the normal range. The other 2 cases of MACS-CPAs were one MACS-CPA_GNAS (MACS-CPA8) and MACS-CPA_no driver (MACS-CPA13). The first case was a 29-year-old female patient with a small ACA of 2 cm (MACS-CPA8), and the second case was a 34-year-old male with a 3.4-cm adrenal nodule (MACS-CPA13), who both failed DST (cortisol levels post-DST 397.3 and 100.2 nmol/L, respectively), and normal 24-hour UFC and ACTH levels. All 3 patients had no clinical signs of CS.

Furthermore, we could distinguish 3 subgroups in Cluster 1 (1A [n = 12], 1B [n = 12], and 1C [n = 8]) and 2 in Cluster 2 (2A [n = 11] and 2B [n = 7]) with a slightly different clinical phenotype (Supplementary Figure 2B (22)). In particular, the homogeneous subcluster 2A includes all 7 CS-CPAs with *PRKACA* mutations and 3 CS-CPAs without driver mutations, together with 1 MACS-CPA_none.

Looking at specifically overexpressed genes in the different clusters (boxes in Fig. 2B), we identified several genes overexpressed in Cluster 2, including *IGFN*1, *CXCL*2, *DPEP*1, *PITX*1, *SHISA*3, *ENC*1, *PLPP*2, *CXCL*14, and *GDF*15. Even if not highlighted in the heatmap, among the most overexpressed genes in Cluster 2, we observed *FATE*1 (Fetal and Adult Testis Expressed 1). Targeted data analysis of *FATE*1 confirmed that CPAs with *GNAS* or *PRKACA* mutations had significantly higher *FATE*1

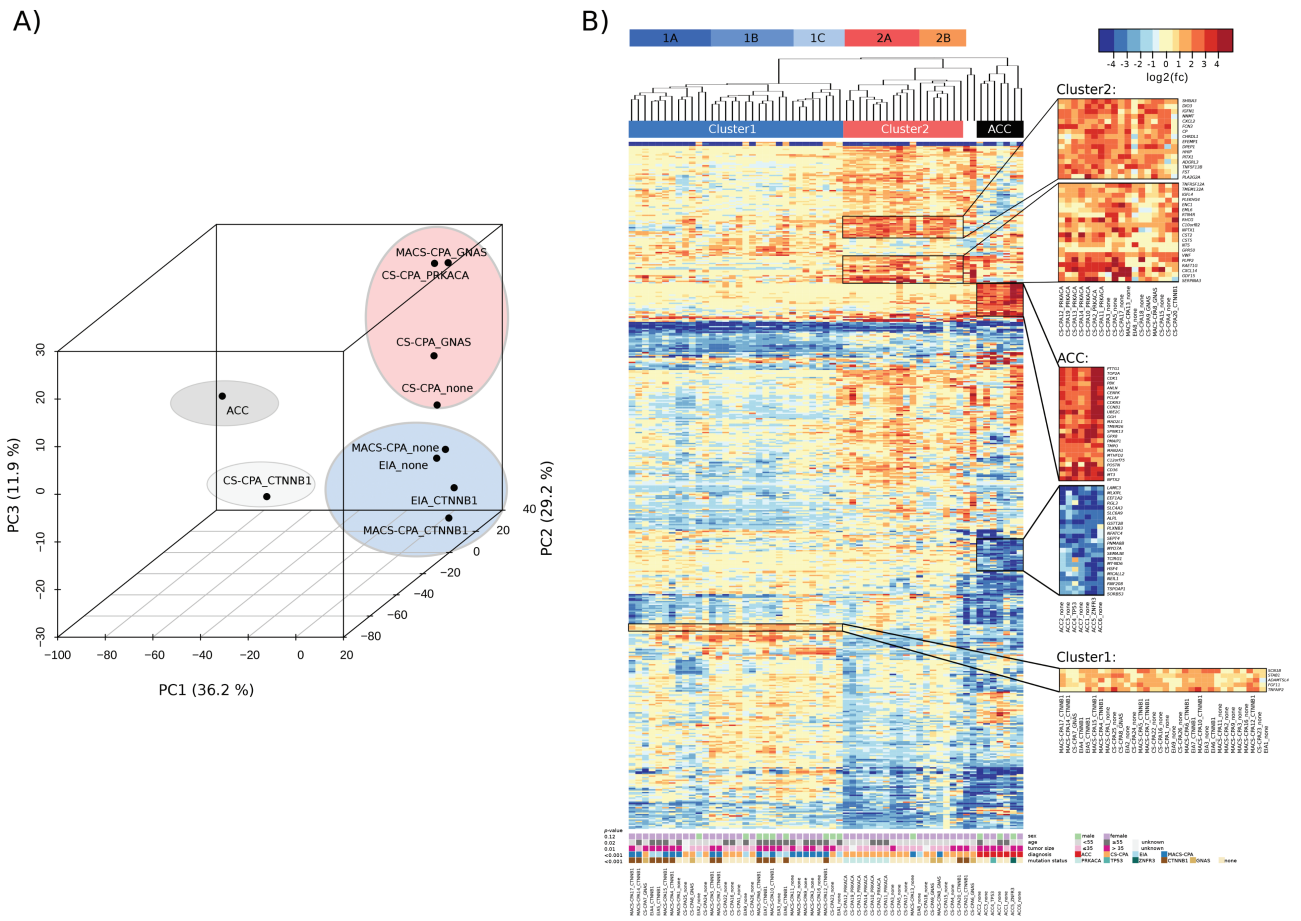

Figure 2. Transcriptome profile analysis of protein-coding genes in adrenocortical tumors. (A) Three-dimensional principal component analysis (3D PCA) and (B) heatmap of the unsupervised clustering analysis for protein-coding genes in adrenocortical carcinomas (ACCs) (n = 7) and adenomas (ACAs, n = 52) divided by functional status according the Endocrine Society guidelines (14) (CS-CPA, cortisol-producing adenoma; MACS-CPA, mild autonomous cortisol secretion; EIA, endocrine-inactive adenoma) as well as mutational status (*PRKACA*, *GNAS* or *CTNNB*1 mutations or no known driver mutations). In the heatmap (B), individual IDs can be seen at the bottom of the figure. Different clusters are recognized and highlighted as Cluster 1 (blue), divided in 1A (n = 12), 1B (n = 12) and 1C (n = 8), and Cluster 2 (red), divided in 2A (n = 11) and 2B (n = 7). Two CS-CPAs (1 with CTNNB1 and 1 with GNAS driver mutation) were not included in the previous clusters. Statistical analysis to evaluate the differences on sex, age (cutoff 50 years old), tumor size (cutoff 3.5 cm), diagnosis (EIA, MACS-CPA, CS-CPA, ACC), and mutation status (no driver vs mutation of cAMP/PKA pathway vs *CTNNB*1 mutation vs other driver mutation) among the clusters was performed using a chi-squared test. $P < .05$ was considered statistically significant. In the boxes, protein-coding genes that are upregulated in Cluster 2 and 1, and genes upregulated or downregulated in ACC, are enlarged. The analysis was performed including the top 500 differentially expressed protein-coding genes using $\log_2$ fold changes in principal components 1, 2, and 3. Color key bar on the top right corner shows $\log_2$ fold changes ($\log_2$(fc)).

mRNA expression than MACS-CPAs or EIAs with or without *CTNNB*1 mutations ($P < .001$ and $P < .01$, respectively) (Fig. 3A). Among Cluster 1, few genes were homogeneously overexpressed, including *STAB*1, *ADAMTSL*4, and *TNFAIP*2 (box in Fig. 2B).

Considering genes related to the steroidogenesis, *NR5A*1 (Nuclear Receptor Subfamily 5 Group A Member 1, known also as steroidogenic factor 1, *SF*1) mRNA expression was significantly lower in ACC than in MACS-CPAs or EIAs with CTNNB1 mutation or without driver mutations ($P < .001$ and $P < .01$, respectively), CS-CPA and MACS-CPA with *GNAS* or *PRKACA* mutation ($P < .001$), or CS-CPA_none ($P < .01$) (Fig. 3A). Of note, CS-CPA with *GNAS* or *PRKACA* mutation showed significantly higher levels of *CYP21A2* than ACC ($P < .001$) and EIA or MACS with *CTNNB*1 driver mutations ($P < .001$), (Fig. 3A). CS-CPA with *GNAS* or *PRKACA* mutation also showed significantly higher levels of *CYP11A1* than ACC as well as EIA or MACS with or without CTNNB1 driver mutations ($P < .001$, $P < .001$, $P < .01$, respectively). ACCs showed also significantly lower levels of several genes encoding for steroidogenic enzymes, including *CYP11B1* and *CYP11B2*, when compared with the remaining tissues (data not shown). No other significant differences could be detected among other groups.

Moreover, genes like *PTTG*1, *TOP2A*, *CDK*1, *CCNB*1, *PBK*, *CDKN*3, *UBE2C*, and *PMAIP*1 were highly expressed selectively in ACC (boxes in Fig. 2B), most of

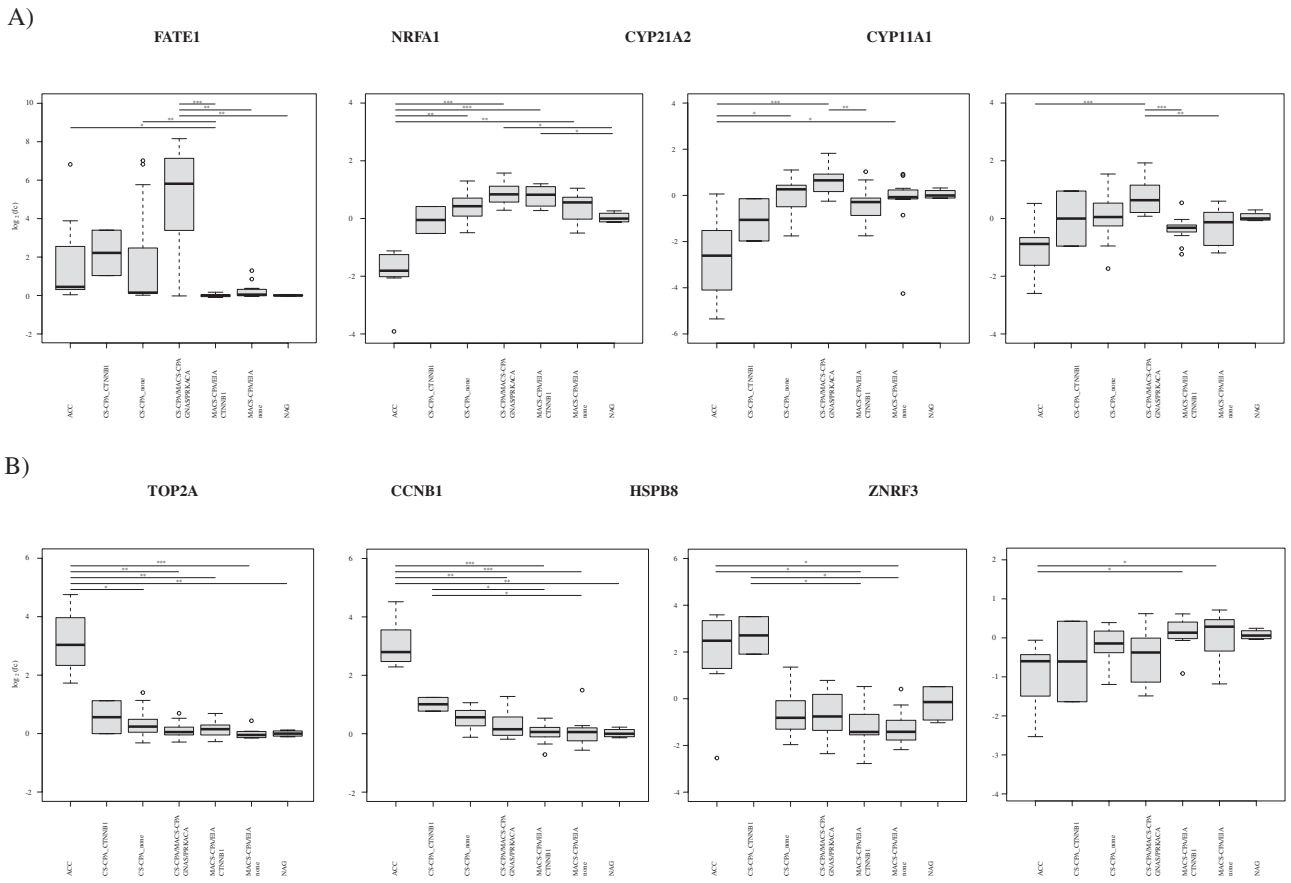

Figure 3. Targeted data analysis evaluating the mRNA expression (log_2FC) of (A) steroidogenic genes *FATE*1, NR5A1, CYP21A2, CYP11A1, and (B) cell cycle–related genes TOP2A, CCNB1, HSPB8, ZNRF3. The samples were grouped in adrenocortical carcinomas (ACC, n = 7) and adrenocortical adenomas (ACAs, n = 52) divided by functional and mutational status: cortisol-producing adenomas (CPAs) associated with Cushing syndrome (CS-CPAs) with *CTNNB*1 mutation (n = 2); mild autonomous cortisol secretion (MACS-CPAs) or endocrine-inactive adenomas (EIAs) with *CTNNB*1 or without driver mutations (n = 13 and n = 12, respectively); CS-CPAs or MACS-CPAs with *PRKACA* or *GNAS* mutations (n = 12); CS-CPA without driver mutations (n = 13). Functional status was evaluated according the Endocrine Society guidelines (14). A nonparametric Kruskal–Wallis test was used significant to detect differences in the distributions of values among groups. The Dunn post hoc analysis was performed using the dunnTest function of R's FSA package, v0.8.23. **P* < 05, ***P* < .01, and****P* <0.001 are statistically significant.

them being involved in cell cycle regulation. Targeted data analysis of *TOP2A* (Topoisomerase 2A) confirmed that ACC had significantly higher mRNA expression than other groups ($P < .001$ compared with MACS-CPAs or EIAs without driver mutation and $P < .01$ compared with ACC with MACS-CPA or EIA with *CTNNB*1 mutation as well as ACC with MACS-CPAs and CS-CPAs with *GNAS* or *PRKACA* mutation, and $P < .05$ when comparing ACC with CS-CPAs_none, Fig. 3B). The analysis of *CCNB*1 (cyclin B1) showed similar results: ($P < .001$ compared with MACS-CPAs or EIAs with *CTNNB*1 or without driver mutation and $P < .01$ comparing ACC with MACS-CPAs and CS-CPAs with *GNAS* or *PRKACA* mutation, respectively, Fig. 3B). Targeted analysis of *HSPB*8, another gene involved in cell proliferation and carcinogenesis, showed higher mRNA levels in both ACC and CS-CPA_CTNNB1 compared with other groups ($P < .05$ compared with MACS-CPA and EIA with or without *CTNNB*1 driver mutation) (Fig. 3B). Moreover, ACC also showed a high number of underexpressed genes, such as *SEPT*4, *SEMA3B*, *GSTT2B*, *HSF*4, and *SORBS*3 (boxes in Fig. 2B). Of note, ACC showed lower mRNA expression of *ZNFR*3 than MACS/EIA_CTNNB1 and EIA/MACS_no driver ($P < .05$) (Fig. 3B). One CPA with *CTNNB*1 mutation and a few cases of EIA/MACS/CPA without driver mutations showed relatively low ZNFR3 levels, even if this was observed also in some CPA with known mutations in cAMP/PKA related genes.

Differential exon usage

We investigated the alternative gene spliced transcripts in all our samples. Comparing the individual groups (ACCs, CS-CPAs, EIAs, MACS-CPAs each against NAGs) according both guidelines (13, 14) no significant differential exon usage was detected (results not shown).

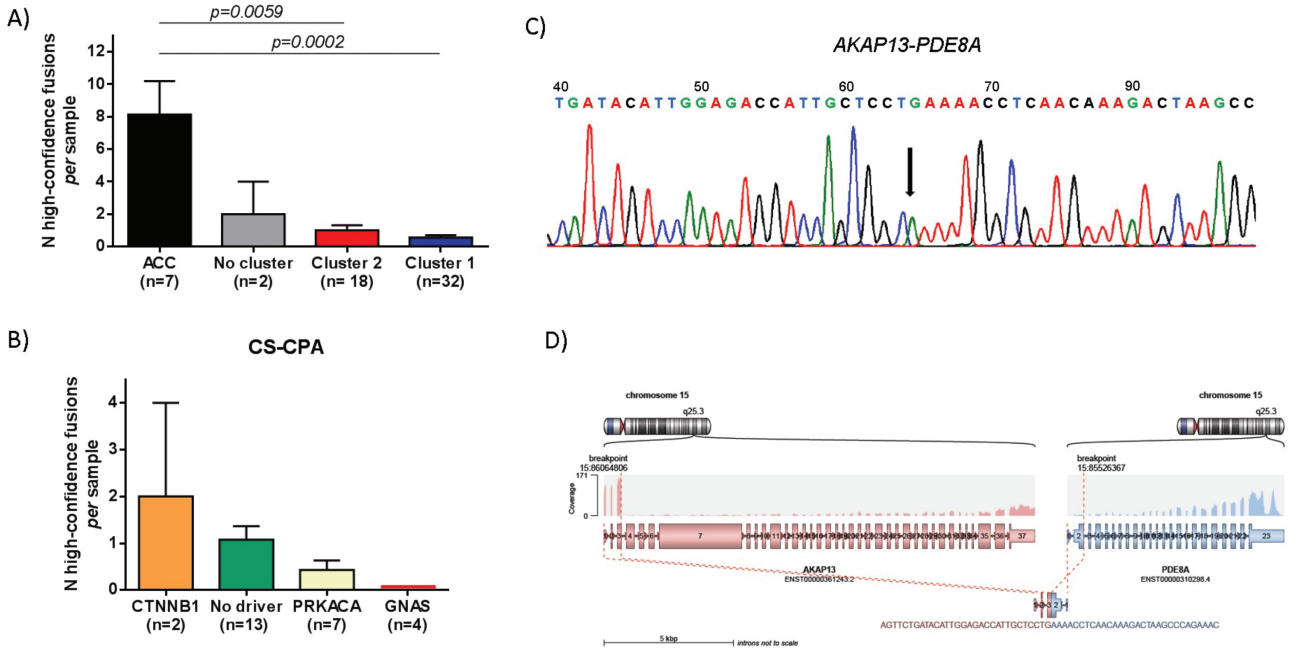

Figure 4. Analysis of gene fusions by RNA-seq in adrenocortical tumors. (A) High-confidence gene fusions recognized at transcriptome profile analysis in adrenocortical carcinomas (ACCs) compared with those found in adenomas associated to Cluster 2 and Cluster 1, and the two cortisol-producing adenoma (CPAs) associated to Cushing syndrome (CS-CPAs) with *CTNNB*1 or GNAS mutation (no cluster). ACCs had a significantly higher number of high-confidence gene fusions than Cluster 2 and 1. (B) High confidence gene fusions among CS-CPAs according to the mutational status, showing that CS-CPA_CTNNB1 had a trend toward a higher number of high-confidence fusions (mean 2.00 ± 2.82) than the other subgroups (mean 1.07 ± 1.04 in CS-CPA_no driver, 0.43 ± 0.53 in CS-CPA_PRKACA). None of the 4 CS-CPA_GNAS had high-confidence gene fusions. In both (A) and (B) the histograms represent the number of fusions ±SEM. Statistical analysis was performed by nonparametric test with Dunn's multiple comparison test. (C) Specific breakpoint of the detected A-kinase anchor protein 13 (*AKAP*13)-phosphodiesterase 8A (*PDE8A*) fusion verified by Sanger sequencing. (D) Predicting fusion by Arriba software including the coding sequence of the *AKAP*13 gene and an intronic sequence of the *PDE8A* gene.

Long noncoding RNA

Several lncRNAs were differentially represented among the groups of tumors. The subgroup PCA confirmed that patients clustered in 4 groups, Supplementary Figure 3A (22): ACCs, CS-CPAs_CTNNB1, 1 group consisting of all EIAs and all MACS-CPA with *CTNNB*1 mutations or without mutation in driver genes, and 1 group consisting of MACS-CPA_GNAS and all the remaining CS-CPAs, in analogy to the results of the coding gene.

At the unsupervised clustering analysis (represented as heatmap in Supplementary Figure 3B (22)) ACCs were clearly differentiated from ACAs, whereas no significant difference arose between the ACA clusters. This could be due to the low number of lncRNAs expressed (n = 384) and the relatively low expression of these genes (Supplementary Table 5 (22)). Only a few lncRNAs were specifically upregulated in ACCs, such as *LINC*01235, *CNRDE*, and *CU*634019.6. The majority of lncRNAs were specifically downregulated in ACCs, including *MEG*3, *CACS*15, *NEAT*1, *DIO*3*OS*, *SPP*14-*AS*1, and *MIR*22*HG* (boxes in Supplementary Figure 3B (22)).

Both PCA and the heatmap for lncRNA showed similar results when we classified the tumors according to the ESE/ENSAT guidelines (13).

Gene fusions

All ACC samples provided evidence for gene fusions. The mean number of high-, medium-, and low-confidence fusions per sample was significantly higher in ACCs than ACAs (8.14 ± 5.43 vs 0.77 ± 1.10 for high-confidence fusions, $P < .0001$; 4.86 ± 227 vs 0.92 ± 1.23 for medium-confidence fusions, $P < .0001$; and 9.57 ± 3.15 vs 3.50 ± 2.32 for low-confidence fusions, $P < .0001$; Supplementary Figure 4 (22)). In contrast, no difference in the number of high-, medium-, and low-confidence gene fusions was observed among CS-CPAs, MACS-CPAs, and EIAs (Supplementary Figure 4 (22)). By considering only high-confidence gene fusions, ACCs had a significantly higher number of fusions per sample than those found in Cluster 1 (0.56 ± 0.75, $P = .0002$) and Cluster 2 (1.0 ± 1.33, $P = .0059$), but not those observed in the 2 CS-CPAs with *CTNNB*1 and *GNAS* mutation that clustered separately (2.0 ± 2.82, $P = .79$; Fig. 4A). After restricting the analysis to CS-CPAs only, there was no significant difference in number of high-confidence fusions per samples considering the mutational status (Fig. 4B). However, CS-CPA_CTNNB1 presented a trend towards higher number of high-confidence fusions compared with other subgroups ($P = .07$; Fig. 4B). We did

not observe any significant difference in number of gene fusions when we classified the tumor according to the ESE/ENSAT guidelines (13).

The entire list of high-confidence gene fusions detected in the present cohort is reported in the Supplementary Table 6 (22). No recurrent fusions were detected in genes involved in cAMP/PKA nor Wnt/beta catenin pathways. However, we identified a "private" fusion between the gene coding for the A-kinase anchor protein 13 (*AKAP*13) and the gene coding the phosphodiesterase 8A (*PDE8A*) in 1 CS-CPA sample without known driver mutations (CS-CPA26; Fig. 4C and 4D). This was validated by PCR. Regarding the other investigated fusions (Supplementary Table 6 (22)), we were able to find 4 out of 6 gene fusions by PCR and Sanger sequencing, including *MAPKAPK5-ACAD*10, *NUP155-WDR*70, *GTF2B-GBP5*, and *SMC6-MSGN*, in the corresponding samples that were positive at RNA-seq. *GADPH*, used as control gene, was found in all the evaluated samples.

Discussion

This is the first study employing RNA-seq to investigate the relationship between transcriptome and the somatic genetic tumor background in a large, well-characterized cohort of benign adrenocortical tumors. We found that transcriptome profiling was able to classify clearly distinct groups that also differed in their hormonal profile and genetic background. Moreover, by applying deep RNA-seq, we identified additional molecular alterations, including gene fusions and differentially expressed lncRNAs associated with the genetic background of the tumors.

The transcriptome profile of benign adrenocortical tumors has been described in a previous publication (20). By applying microarray analysis on a small number of ACAs (n = 22), Wilmout Roussel and colleagues identified a specific molecular signature of CS-CPAs, different from that of EIAs or MACS-CPAs, which clustered together. The results of the unsupervised clustering analysis performed in our study partly confirms those findings, showing that most benign adrenocortical tumors could be divided in 2 groups, named Cluster 1, including mostly EIAs and MACS-CPAs, and Cluster 2, comprising mostly CS-CPAs. The clinical features of patients in the 2 clusters revealed that patients in Cluster 2 were mostly young females, with small hyperfunctioning tumors, whereas those in Cluster 1 had mostly inactive or "low-functional" large tumors. Therefore, MACS-CPAs and EIAs samples, together with a subgroup of CS-CPA_no driver and _GNAS, showed a similar transcriptome profile, which was clearly different from that of most CS-CPAs and ACCs. Those findings are consistent with previous clinical observations, showing that MACS-CPA tumors seem to be a separate clinical entity from overt CS. Although patients with MACS-CPA could present comorbidities associated to mild cortisol hypersecretion, such as risk of cardiovascular events, hypertension, dyslipidemia, diabetes mellitus type 2, obesity, osteoporosis (13, 15-19), the long-term data did not provide evidence for an evolution from MACS-CPA to overt CS (32). Additionally, recent analysis by liquid chromatography tandem mass spectrometry in patients with adrenal incidentalomas showed that the steroid profiling of subjects with EIA showed some similarities with those having MACS-CPA (33, 34).

The combined analysis of transcriptome profiling with a tumor whole genome background performed in our cohort allowed us to pinpoint additional important findings. The similar transcriptome profile of MACS-CPA and EIA samples was independent of the presence of *CTNNB*1 mutations, which were the most common alterations detected in tumors of this group. Additionally, the similar transcriptome profile among CS-CPAs is consistent with the activation of the cAMP/PKA pathway, independently of the underlying putative mutation.

Among differentially expressed genes, it is worth mentioning *FATE*1 as the most overexpressed gene in tumors belonging to Cluster 2, and specifically, in CS-CPAs samples carrying *PRKACA* and *GNAS* somatic mutations. *FATE*1 encodes a known transcription factor involved in regulation of apoptosis and cell proliferation, regulated by steroidogenic factor 1 (SF1) at the promoter level (35). Considering the pivotal role of SF1 in steroid producing cells and the interplay between FATE1 and SF1 (36), our data provide additional evidence for the molecular events caused by cAMP/PKA pathway disruption due to *PRKACA* and *GNAS* somatic mutations at a transcriptional level.

Considering that the most evident difference between Cluster 1 and Cluster 2 is the steroid secreting pattern, we analyzed the expression of several genes involved in steroidogenesis. In particular, we could confirm that the expression of genes encoding for key enzymes such as CYP11A1 (cytochrome P450 cholesterol monooxigenase) and CYP21A2 (21-hydroxylase) was significantly higher in CPAs carrying mutations in the cAMP-PKA genes than both ACC and EIA/MACS-CPA with CTNNB1 mutations. These data are consistent with the hyperactivation of cAMP-PKA pathway observed in tumors carrying such mutations, driving the activation of the steroidogenic cascade (37).

Considering the individual 3D PCA for all protein-coding genes, the mRNA expression profile of the subgroup of CS-CPAs associated with *CTNNB*1 mutations was more similar to that of ACCs than the remaining CS-CPAs or tumors included in Cluster 1, which were mostly carrying *CTNNB*1 mutations. However, when analyzed at an

individual level of the transcriptome profiling at unsupervised clustering for protein-coding genes, CS-CPAs with *CTNNB1* mutations showed heterogeneity: one sample clustered in Cluster 2, whereas the other sample clustered separately together with a CS-CPA_GNAS closely to ACCs. The discrepancy between the 3D PCA and the unsupervised clustering analysis could be related by the low number of CS-CPA with *CTNNB1* mutation in our cohort (n = 2) and by the significantly different number of genes evaluated in the two analyses. Notably, *TOP2A*, the gene encoding Topoisomerase II Alpha, was among the overexpressed genes in both CS-CPA samples with *CTNNB1* mutations and ACCs, different from the remaining benign tumors. TOP2A is a cell cycle–related protein, involved in cell proliferation by controlling the topologic states of DNA during transcription in several types of cancer and is being studied as a potential druggable target for several anticancer agents (38). Several studies in ACC tissues have shown an overexpression of *TOP2A*, which was tightly correlated with Ki67, a marker of cell proliferation, and poor survival (39, 40). Taken together, those observations reinforce the hypothesis proposed in several previous studies of a potential adenoma-carcinoma sequence in a subgroup of adrenocortical tumors. Indeed, studies on animal models and human tissues have shown that alterations of the Wnt-beta catenin pathway, IGF2 signaling and Notch signaling may boost the transformation of an ACA into ACC (41-43). Even though such an event is exceedingly rare (44), the alterations identified in benign adrenocortical tumors described in our study and in previous investigations may represent a preliminary phase in the multistep potential evolution towards ACC.

The analysis of lncRNAs provided interesting insights into the molecular signature of adrenocortical tumors. LncRNAs are noncoding RNA transcripts >200 nucleotides in length, involved in epigenetic silencing, regulation of splicing and transcription (45). LncRNAs dysregulation has been described as a potential marker of ACC, with clinical implications. Recent studies have shown that the lncRNA molecular signature may discriminate ACCs from ACAs and NAGs and identify patients affected by ACC with poor prognosis (46, 47). Our lncRNA signature analysis confirmed those previous results (46, 47), underlining that most lncRNAs are downregulated in ACCs. We demonstrated that among benign tumors there were no significant difference in lncRNA expression between the clusters, although at 3D-PCA analysis for lncRNAs, CS-CPAs_CTNNB1 were separated from the rest of adenomas.

The analysis of fusion genes, performed in benign adrenocortical tumors for the first time, showed that CS-CPAs samples carrying *CTNNB1* mutations had a number of high-confidence gene fusions that was set in between ACCs and remaining CS-CPAs. Previous studies have identified fusion transcripts, a product of chromosomal rearrangements, as useful markers for several hematological malignancies and epithelial cancers, with important implications in treatment strategies (48). In our study, we demonstrated for the first time that ACCs had a significantly higher number of gene fusions compared with all ACAs. A recent pangenomic characterization of ACCs has described a few private fusion transcripts, namely *EXOSC10-MTOR* and *MLL-ATP5L*, involving genes with well-known roles in cancer development (49), even though the impact of those events in the pathogenesis of ACC should be confirmed by further targeted studies. The results of the analysis of fusion transcripts in our cohort reinforce the hypothesis that CS-CPAs with *CTNNB1* mutations may have a different biological behavior than the remaining functioning and nonfunctioning benign adrenocortical tumors. As an additional interesting finding, we could identify the fusion transcript *AKAP13-PDE8A* in one case of CS-CPA without known driver somatic mutations. In a recent study, a similar fusion transcript has been frequently detected in colorectal cancer (50). The predicted PDE8A protein retained the conserved catalytic domain located at the C-terminal region, leading to the hypothesis that the promoter region of AKAP13, which is an A-kinase anchoring protein, might alter cAMP signaling through PDE8A dysregulation (50). Considering the involvement of phosphodiesterases in the pathogenesis of Cushing syndrome (51), the involvement of *AKAP13-PDE8A* fusion transcript in the pathogenesis of a subset of CS-CPAs without driver mutations at WES is an intriguing mechanism that should be investigated in future functional studies.

The main limitation of this study is represented by the rather small number of patients in selected groups of interest, which may limit the interpretation of the results and the possibility to perform correlations between transcriptome and clinical data. Nonetheless, this is the result of a strict selection process that relied on the genetic mutations identified in previous studies (6, 9) and availability of high-quality RNA for RNA-seq. To avoid bias in the evaluation of our results, we performed the analysis following the definition of MACS-CPA and CS-CPA according to both the Endocrine Society and the ESE/ENSAT guidelines (13, 14). The classification of three samples changes between the two guidelines: 2 MACS-CPAs without driver mutations, which are classified as EIAs according to the newest ESE/ENSAT guidelines, and 1 EIA with *CTNNB1* mutation MACS-CPS that was reclassified as EIA. By comparing the results, we found few differences only in the protein-coding heatmap, where CS-CPAs without known driver mutations do not cluster together with the CS-CPA with *GNAS* or *PRKACA* mutation as previously. In our opinion, this difference depends on the relatively low number of cases in

some diagnostic groups, leading to small changes in gene expression patterns and different clustering. Moreover, gene fusions, PCA, and heatmaps for lncRNA genes do not change between the tumor classification according the two guidelines. Therefore, we decide to show into details the results obtained by classifying the tumor according to the Endocrine Society guidelines, in order to keep the same tumor classification of the previous studies (6, 9), allowing a better characterization of the tumor samples.

Another possible explanation for the mutation-negative cases might be the sensitivity of sequencing methods in detecting mutations with low allele frequencies, as shown in recent studies highlighting the possibility of increasing the detection of mutations by applying targeted immunohistochemistry-driven deep sequencing in primary aldosteronism (52). Moreover, due the limitation of the methods, large insertions, deletions as well as methylation aberrations were not analyzed by WES and, therefore, they might have been missed. Nonetheless, our retrospective cohort of fresh-frozen tumors was heterogeneous, and an immunohistochemistry-driven approach would not have been possible. Finally, another limitation of our study is that tumors were dissected macroscopically. Therefore, even though the procedure was made by pathologists, our analysis may carry the chance of sampling error, in analogy to other studies dealing with snap-frozen tissues. More accurate data may derive by an in situ methodology, such as laser-capture microdissection. The strength of our study is that the characterization of transcriptome profile and additional RNA alterations (gene fusions and differential expression of lncRNA) is evaluated in a large cohort of adrenocortical tumors (n = 59) and analyzed according to both the functional status and the presence of driver mutations.

Conclusion

In conclusion, our findings suggest that still unrevealed molecular modifications (in cAMP/PKA pathway) might be involved in the pathogenesis of autonomous steroid secretion, some of them depending on the underlying genetic background. At variance, MACS-CPAs seem to be molecularly related to EIAs, independently from the genetic background. Finally, the slightly similarity of molecular alterations between CS-CPAs carrying *CTNNB1* mutations and ACCs may pave the way for further targeted investigation aimed at defining the potential adenoma-carcinoma sequence in adrenocortical tumors.

Acknowledgments

The authors are grateful to Mrs. Sonja Steinhauer and Ms. Martina Zink for excellent technical support and Ms. Michaela Haaf for coordinating the ENSAT Registry. This work has been carried out with the help of the Interdisciplinary Bank of Biomaterials and Data of the University Hospital of Wuerzburg and the Julius Maximilian University of Wuerzburg (IBDW). The implementation of the IBDW has been supported by the Federal Ministry for Education and Research (Grant number FKZ: 01EY1102).

Financial Support: This work has been supported by the Deutsche Forschungsgemeinschaft (DFG) within the CRC/Transregio (project number: 314061271 – TRR 205 to A.R., A.O., F.B., M.F., and C.L.R.), and project FA-466/8-1 and RO-5435/3-1 (M.F and C.L.R., respectively), the Deutsche Krebshilfe (70113526 S.A., M.F. and C.L.R., and 70112617 to F.B. and M.F.), the Else Kröner-Fresenius-Stiftung (2015_A228 to A.R.), the Italian Ministry of Health (RF-GR-2018-12365398 to G.D.D. and RF-2013-02356606 to I.C.), the Italian Ministry of University and Research (PRIN 2017 to G.D.D.).

Additional information

Correspondence and Reprint Requests: Cristina L Ronchi, MD, PhD, Division of Endocrinology and Diabetes, Department of Internal Medicine I, University Hospital, University of Würzburg, Oberduerrbacher-Str 6, 97080, Würzburg, Germany. E-Mail: Ronchi_C@ukw.de.

Disclosure Summary: The authors have nothing to disclose.

Data Availability: The raw data have been uploaded into the platform EGA (https://www.ebi.ac.uk/ega/home, accession number EGAS00001004533). Further datasets analyzed during the current study are available from the corresponding author on reasonable request.

References

1. Di Dalmazi G. *Cushing Syndrome-Unilateral Adrenal Adenoma. Encyclopedia of Endocrine Diseases*. Module in Biomedical Sciences. 2nd ed. Academic Press; 2018:4252.
2. Ronchi CL. cAMP/protein kinase A signalling pathway and adrenocortical adenomas. *Curr Opin Endocr Metab Res*. 2019;**8**:15-21.
3. Beuschlein F, Fassnacht M, Assié G, et al. Constitutive activation of PKA catalytic subunit in adrenal Cushing's syndrome. *N Engl J Med*. 2014;**370**(11):1019-1028.
4. Cao Y, He M, Gao Z, et al. Activating hotspot L205R mutation in PRKACA and adrenal Cushing's syndrome. *Science*. 2014;**344**(6186):913-917.
5. Goh G, Scholl UI, Healy JM, et al. Recurrent activating mutation in PRKACA in cortisol-producing adrenal tumors. *Nat Genet*. 2014;**46**(6):613-617.
6. Di Dalmazi G, Kisker C, Calebiro D, et al. Novel somatic mutations in the catalytic subunit of the protein kinase A as a cause of adrenal Cushing's syndrome: a European multicentric study. *J Clin Endocrinol Metab*. 2014;**99**(10):E2093-E2100.
7. Sato Y, Maekawa S, Ishii R, et al. Recurrent somatic mutations underlie corticotropin-independent Cushing's syndrome. *Science*. 2014;**344**(6186):917-920.
8. Espiard S, Knape MJ, Bathon K, et al. Activating PRKACB somatic mutation in cortisol-producing adenomas. *JCI Insight*. 2018;**3**(8):e98296.
9. Ronchi CL, Di Dalmazi G, Faillot S, et al.; European Network for the Study of Adrenocortical Tumors (ENSAT). Genetic

landscape of sporadic unilateral adrenocortical adenomas without PRKACA p.Leu206Arg mutation. *J Clin Endocrinol Metab*. 2016;**101**(9):3526-3538.
10. Bathon K, Weigand I, Vanselow JT, et al. Alterations in protein kinase a substrate specificity as a potential cause of Cushing syndrome. *Endocrinology*. 2019;**160**(2):447-459.
11. Tissier F, Cavard C, Groussin L, et al. Mutations of beta-catenin in adrenocortical tumors: activation of the Wnt signaling pathway is a frequent event in both benign and malignant adrenocortical tumors. *Cancer Res*. 2005;**65**(17):7622-7627.
12. Bonnet S, Gaujoux S, Launay P, et al. Wnt/β-catenin pathway activation in adrenocortical adenomas is frequently due to somatic CTNNB1-activating mutations, which are associated with larger and nonsecreting tumors: a study in cortisol-secreting and -nonsecreting tumors. *J Clin Endocrinol Metab*. 2011;**96**(2):E419-E426.
13. Fassnacht M, Arlt W, Bancos I, et al. Management of adrenal incidentalomas: European Society of Endocrinology Clinical Practice Guideline in collaboration with the European Network for the Study of Adrenal Tumors. *Eur J Endocrinol*. 2016;**175**(2):G1-G34.
14. Nieman LK, Biller BM, Findling JW, et al. The diagnosis of Cushing's syndrome: an Endocrine Society Clinical Practice Guideline. *J Clin Endocrinol Metab*. 2008;**93**(5):1526-1540.
15. Di Dalmazi G, Vicennati V, Garelli S, et al. Cardiovascular events and mortality in patients with adrenal incidentalomas that are either non-secreting or associated with intermediate phenotype or subclinical Cushing's syndrome: a 15-year retrospective study. *Lancet Diabetes Endocrinol*. 2014;**2**(5):396-405.
16. Di Dalmazi G, Vicennati V, Rinaldi E, et al. Progressively increased patterns of subclinical cortisol hypersecretion in adrenal incidentalomas differently predict major metabolic and cardiovascular outcomes: a large cross-sectional study. *Eur J Endocrinol*. 2012;**166**(4):669-677.
17. Altieri B, Muscogiuri G, Paschou SA, et al. Adrenocortical incidentalomas and bone: from molecular insights to clinical perspectives. *Endocrine*. 2018;**62**(3):506-516.
18. Reimondo G, Castellano E, Grosso M, et al. Adrenal incidentalomas are tied to increased risk of diabetes: findings from a prospective study. *J Clin Endocrinol Metab*. 2020;**105**(4). doi: 10.1210/clinem/dgz284.
19. Athimulam S, Delivanis D, Thomas M, et al. The impact of mild autonomous cortisol secretion on bone turnover markers. *J Clin Endocrinol Metab*. 2020;**105**(5):1469-1477.
20. Wilmot Roussel H, Vezzosi D, Rizk-Rabin M, et al. Identification of gene expression profiles associated with cortisol secretion in adrenocortical adenomas. *J Clin Endocrinol Metab*. 2013;**98**(6):E1109-E1121.
21. Lippert J, Appenzeller S, Liang R, et al. Targeted molecular analysis in adrenocortical carcinomas: a strategy toward improved personalized prognostication. *J Clin Endocrinol Metab*. 2018;**103**(12):4511-4523.
22. Di Dalmazi G, Altieri B, Scholz C, et al. Data from: RNA-Sequencing and Somatic Mutation Status of Adrenocortical Tumors: Novel Pathogenetic insights. OSF - Open Science Framework 2020. Deposited August 17, 2020. ProMED-mail website. https://osf.io/fhqay.
23. Martin M. Cutadapt removes adapter sequences from high-throughput sequencing reads. *EMBnetjournal*. 2011;**17**(1):10-12.
24. Dobin A, Davis CA, Schlesinger F, et al. STAR: ultrafast universal RNA-seq aligner. *Bioinformatics*. 2013;**29**(1):15-21.
25. Li H, Handsaker B, Wysoker A, et al.; 1000 Genome Project Data Processing Subgroup. The Sequence Alignment/Map format and SAMtools. *Bioinformatics*. 2009;**25**(16):2078-2079.
26. Trapnell C, Williams BA, Pertea G, et al. Transcript assembly and quantification by RNA-Seq reveals unannotated transcripts and isoform switching during cell differentiation. *Nat Biotechnol*. 2010;**28**(5):511-515.
27. Subramanian A, Tamayo P, Mootha VK, et al. Gene set enrichment analysis: a knowledge-based approach for interpreting genome-wide expression profiles. *Proc Natl Acad Sci U S A*. 2005;**102**(43):15545-15550.
28. Mootha VK, Lindgren CM, Eriksson KF, et al. PGC-1alpha-responsive genes involved in oxidative phosphorylation are coordinately downregulated in human diabetes. *Nat Genet*. 2003;**34**(3):267-273.
29. McKenna A, Hanna M, Banks E, et al. The Genome Analysis Toolkit: a MapReduce framework for analyzing next-generation DNA sequencing data. *Genome Res*. 2010;**20**(9):1297-1303.
30. Wang K, Li M, Hakonarson H. ANNOVAR: functional annotation of genetic variants from high-throughput sequencing data. *Nucleic Acids Res*. 2010;**38**(16):e164.
31. Altieri B, Sbiera S, Della Casa S, et al. Livin/BIRC7 expression as malignancy marker in adrenocortical tumors. *Oncotarget*. 2017;**8**(6):9323-9338.
32. Elhassan YS, Alahdab F, Prete A, et al. Natural history of adrenal incidentalomas with and without mild autonomous cortisol excess: a systematic review and meta-analysis. *Ann Intern Med*. 2019;**171**(2):107-116.
33. Di Dalmazi G, Fanelli F, Mezzullo M, et al. Steroid profiling by LC-MS/MS in nonsecreting and subclinical cortisol-secreting adrenocortical adenomas. *J Clin Endocrinol Metab*. 2015;**100**(9):3529-3538.
34. Di Dalmazi G, Fanelli F, Zavatta G, et al. The steroid profile of adrenal incidentalomas: subtyping subjects with high cardiovascular risk. *J Clin Endocrinol Metab*. 2019;**104**(11):5519-5528.
35. Doghman M, Karpova T, Rodrigues GA, et al. Increased steroidogenic factor-1 dosage triggers adrenocortical cell proliferation and cancer. *Mol Endocrinol*. 2007;**21**(12):2968-2987.
36. Doghman-Bouguerra M, Granatiero V, Sbiera S, et al. FATE1 antagonizes calcium- and drug-induced apoptosis by uncoupling ER and mitochondria. *EMBO Rep*. 2016;**17**(9):1264-1280.
37. Miller WL, Auchus RJ. The molecular biology, biochemistry, and physiology of human steroidogenesis and its disorders. *Endocr Rev*. 2011;**32**(1):81-151.
38. Lee JH, Berger JM. Cell cycle-dependent control and roles of DNA topoisomerase II. *Genes (Basel)*. 2019;**10**(11):859.
39. Jain M, Zhang L, He M, Zhang YQ, Shen M, Kebebew E. TOP2A is overexpressed and is a therapeutic target for adrenocortical carcinoma. *Endocr Relat Cancer*. 2013;**20**(3):361-370.
40. Gupta D, Shidham V, Holden J, Layfield L. Value of topoisomerase II alpha, MIB-1, p53, E-cadherin, retinoblastoma gene protein product, and HER-2/neu immunohistochemical expression for the prediction of biologic behavior in adrenocortical neoplasms. *Appl Immunohistochem Mol Morphol*. 2001;**9**(3):215-221.
41. Heaton JH, Wood MA, Kim AC, et al. Progression to adrenocortical tumorigenesis in mice and humans through

insulin-like growth factor 2 and β-catenin. *Am J Pathol*. 2012;**181**(3):1017-1033.
42. Drelon C, Berthon A, Ragazzon B, et al. Analysis of the role of Igf2 in adrenal tumour development in transgenic mouse models. *PLoS One*. 2012;**7**(8):e44171.
43. Ronchi CL, Sbiera S, Leich E, et al. Single nucleotide polymorphism array profiling of adrenocortical tumors–evidence for an adenoma carcinoma sequence? *PLoS One*. 2013;**8**(9):e73959.
44. Belmihoub I, Silvera S, Sibony M, et al. From benign adrenal incidentaloma to adrenocortical carcinoma: an exceptional random event. *Eur J Endocrinol*. 2017;**176**(6):K15-K19.
45. Morris KV, Mattick JS. The rise of regulatory RNA. *Nat Rev Genet*. 2014;**15**(6):423-437.
46. Glover AR, Zhao JT, Ip JC, et al. Long noncoding RNA profiles of adrenocortical cancer can be used to predict recurrence. *Endocr Relat Cancer*. 2015;**22**(1):99-109.
47. Buishand FO, Liu-Chittenden Y, Fan Y, et al. Adrenocortical tumors have a distinct, long, non-coding RNA expression profile and LINC00271 is downregulated in malignancy. *Surgery*. 2020;**167**(1):224-232.
48. Neckles C, Sundara Rajan S, Caplen NJ. Fusion transcripts: Unexploited vulnerabilities in cancer? *Wiley Interdiscip Rev RNA*. 2020;**11**(1):e1562.
49. Zheng S, Cherniack AD, Dewal N, et al.; Cancer Genome Atlas Research Network. Comprehensive pan-genomic characterization of adrenocortical carcinoma. *Cancer Cell*. 2016;**30**(2):363.
50. Nome T, Thomassen GO, Bruun J, et al. Common fusion transcripts identified in colorectal cancer cell lines by high-throughput RNA sequencing. *Transl Oncol*. 2013;**6**(5):546-553.
51. Leal LF, Szarek E, Faucz F, Stratakis CA. Phosphodiesterase 8B and cyclic AMP signaling in the adrenal cortex. *Endocrine*. 2015;**50**(1):27-31.
52. Nanba AT, Wannachalee T, Shields JJ, et al. Adrenal vein sampling lateralization despite mineralocorticoid receptor antagonists exposure in primary aldosteronism. *J Clin Endocrinol Metab*. 2019;**104**(2):487-492.